Available online at www.sciencedirect.com
SCIENCE DIRECT®
Pergamon
Cement and Concrete Research 33 (2003) 1949–1962
CEMENT AND CONCRETE RESEARCH

Specimen preparation and image processing and analysis techniques for automated quantification of concrete microcracks and voids

Parviz Soroushian[a,*], Mohamed Elzafraney[a], Ali Nossoni[b]

[a]*Civil and Environmental Engineering Department, Michigan State University, 3546 Engineering Building, East Lansing, MI 48824-1226, USA*
[b]*DPD, Inc., USA*

Received 22 August 2002; accepted 9 June 2003

Abstract

Specimen preparation and image processing/analysis techniques were developed for use in automated quantitative microstructural investigation of concrete, focusing on concrete microcracks and voids. Different specimen preparation techniques were developed for use in fluorescent and scanning electron microscopy (SEM) of concrete; then techniques produce a sharp contrast between microcracks/voids and the body of concrete. The image processing/analysis techniques developed specifically for use with concrete address the following usages: automatic threshold; development of intersecting microcracks/voids and connected voids; distinction of microcracks form voids based on geometric attributes; and noise filtration.

Keywords: Concrete; Specimen preparation; Microscopy; Image processing; Image analysis

1. Introduction

Different damaging effects yield different levels and configurations of microcrack propagation in concrete, which, in turn, influence the post-damage behaviors and qualities of concrete [1,2]. Quantitative investigation of the microcracks system in concrete can thus provide substantial insight into the deterioration and failure processes of the concrete-based infrastructure. Latest developments in microscopy and image processing techniques have facilitated efforts towards investigation of the concrete microstructure [3,4]. Given the complexity and heterogeneity of the concrete structure, development of statistically reliable quantitative information about concrete microstructure requires acquisition, processing, and analysis of a relatively large number of microscopic images. Automation of image processing and analysis procedures can facilitate practical use of modern image analysis schemes in quantitative microstructural analysis of concrete towards development of valuable structure–property relationships for concrete. General proper image processing and analysis techniques involve diverse and complex routines; practical use of these techniques with concrete requires tailoring of such routines to suit concrete microstructure. Preparation of concrete samples so that the feature of interest (microcracks and voids) develop a distinct contrast against the body of concrete in the selected microscopy technique is the prerequisite for application of modern automated image processing and analysis techniques to concrete microscopic images [5]. Specimen preparation method depends generally on the type of microscopy used [6]. Removal of noise and distinction of microcracks from voids are also important for the purpose of automation and quantification [5]. Once the features of interest are distinguished, meaningful quantitative date should be produced which reflect on engineering properties of concrete and provide a basis for development of structure–property relationships. The work reported herein establishes specimen preparation techniques for automated investigation of concrete microcracks and voids through scanning electron microscopy (SEM) and also through fluorescent microscopy. Image processing and analysis routines are also developed for removal of noise, distinction of microcracks from voids, and detachment of connected microcracks and voids in concrete micrographs.

* Corresponding author. Tel./fax: +1-517-355-2216.
E-mail address: soroushi@egr.msu.edu (P. Soroushian).

0008-8846/$ – see front matter © 2003 Elsevier Ltd. All rights reserved.
doi:10.1016/S0008-8846(03)00219-9

2. Specimen preparation techniques

The objectives of specimen preparation for microscopic analysis are to provide a finely ground and polished surface which yield crisp images and sharp edges with good differentiation between the features of interest (microcracks and voids in this study) and the body of concrete. Selection of a specimen preparation technique depends on the objects (features) of interest and the microscopy technique. The "red dye" impregnation technique [7], for example, has been used to prepare concrete specimens for optic microscopy. This technique, however, fails to satisfactorily distinguish cracks from porous zones of the paste [8]. For the purpose of environmental scanning electron microscopy (ESEM) or conventional scanning electron microscopy (SEM), satisfactory results have been reported for concrete specimens impregnated with Wood's metal [9,10]. This approach yields a desirable contrast between features of interest (microcracks and voids) and the background. Concerns have been expressed that lapping and polishing processes which usually accompany with Wood's metal impregnation may lead to incorrect diagnoses of concrete components (e.g., in the case of concrete damaged by delayed ettringite formation) [6]. Special care is needed in the selection of variables such as temperature and pressure during Wood's metal impregnation. For fluorescent microscopy, the most common method of specimen preparation involves epoxy impregnation [11]. Epoxy impregnation can highlight more porous areas of cement paste, but it is not effective in distinguishing cracks. Epoxy impregnation does not generally yield crisp boundaries and sharp contrast between microcracks and air voids versus the body of concrete. The fluorescent liquid technique "which has been used to improve conventional epoxy impregnation; while this technique shows promise, it involves time-consuming immersion of concrete specimens in fluorescent and ethanol solution for several days, and its application is limited to the research reported herein" improved the Wood's metal impregnation technique for (environmental) scanning electron microscopy (by backscattered technique) and also developed a new two-stage (ink–epoxy) impregnation technique for preparation of concrete samples for the purpose of fluorescent microscopy.

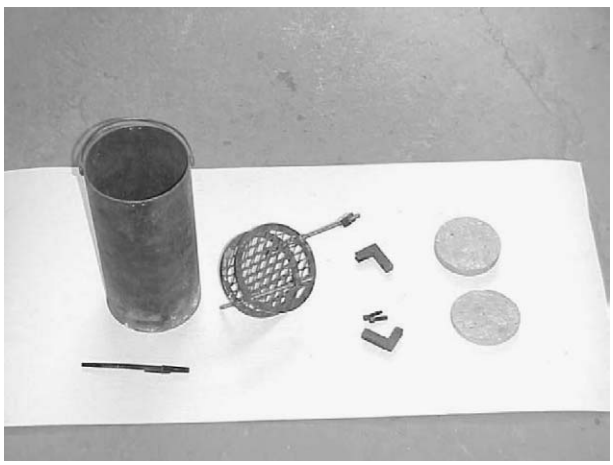

Fig. 1. Steel container used for Wood's metal specimen preparation.

Fig. 2. Placing the metal container containing concrete specimen in the pressure chamber.

2.1. Specimen preparation for ESEM (Wood's metal impregnation)

The preparation starts by cutting the specimen into 50.8-mm (2-in.)-thick slices using a suitable electrical saw. The sections should provide the maximum planar dimensions allowed by the original specimen size, steel container dimensions, and microscope chamber and travel stage. The cut sections are then washed using liquid soap and tap water in order to remove any debris attached to the specimen during the cutting process. The sections are then dried in an electrical oven at 65 °C (150 °F) for 24 h to remove any water inside the specimen that may encumber the impregnation process. The dried sections are placed in a steel mold for the purpose of Wood's metal impregnation. The diameter of the steel container is 140 mm (5.5 in.), and its height is 54 mm (10 in.). This particular container has movable perforated steel shelves to accommodate multiple sections as shown in Fig. 1. Wood's metal is added to the steel container at 12 times the weight of concrete sections. The used Wood's metal melts at 70 °C (158 °F) and is solid in dry air at room temperature 20 °C (68 °F); it consists of 50% bismuth (Bi), 25% lead (Pb), 12.5% cadmium (Cd), and 12.5% tin (Sn). The Wood's metal has a Young's modulus of 9.7 GPa (1,400,000 psi), a density of 9.67 g/cm^3 (600 lb/ft^3), and does not go through any volume change during hardening [12]. The container incorporating concrete sections and Wood's metal is placed inside a pressure chamber as shown in Fig. 2. The pressure chamber should have capabilities for vacuum and pressured nitrogen gas application and also for heating. The air inside the chamber is removed by turning the vacuum on to 6.65 kPa (0.95 psi) for 30–40 min. Next, the chamber is heated

(under vacuum) to 93 °C (200 °F) for 1–2 h in order to allow for Wood's metal melting. Subsequently, vacuum is turned off (with heat still on), and the chamber is subjected to nitrogen gas at pressure of 1.94–2 MPa (280–300 psi) for 3–4 h in order to allow Wood's metal to penetrate the concrete. After turning the pressure and heat off, the specimen is allowed to cool down to room temperature while concrete sections are immersed in Wood's metal. Once the chamber reaches room temperature, 6 mm (0.25 in.) is cut off the surface layer of the specimen in the required direction by electrical saw in order to expose an impregnated concrete surface. The specimen is then polished using polishing machine and consecutive sets of 320, 600, 1200, and 4000 grit 5–7 min each at 300 rpm silicon

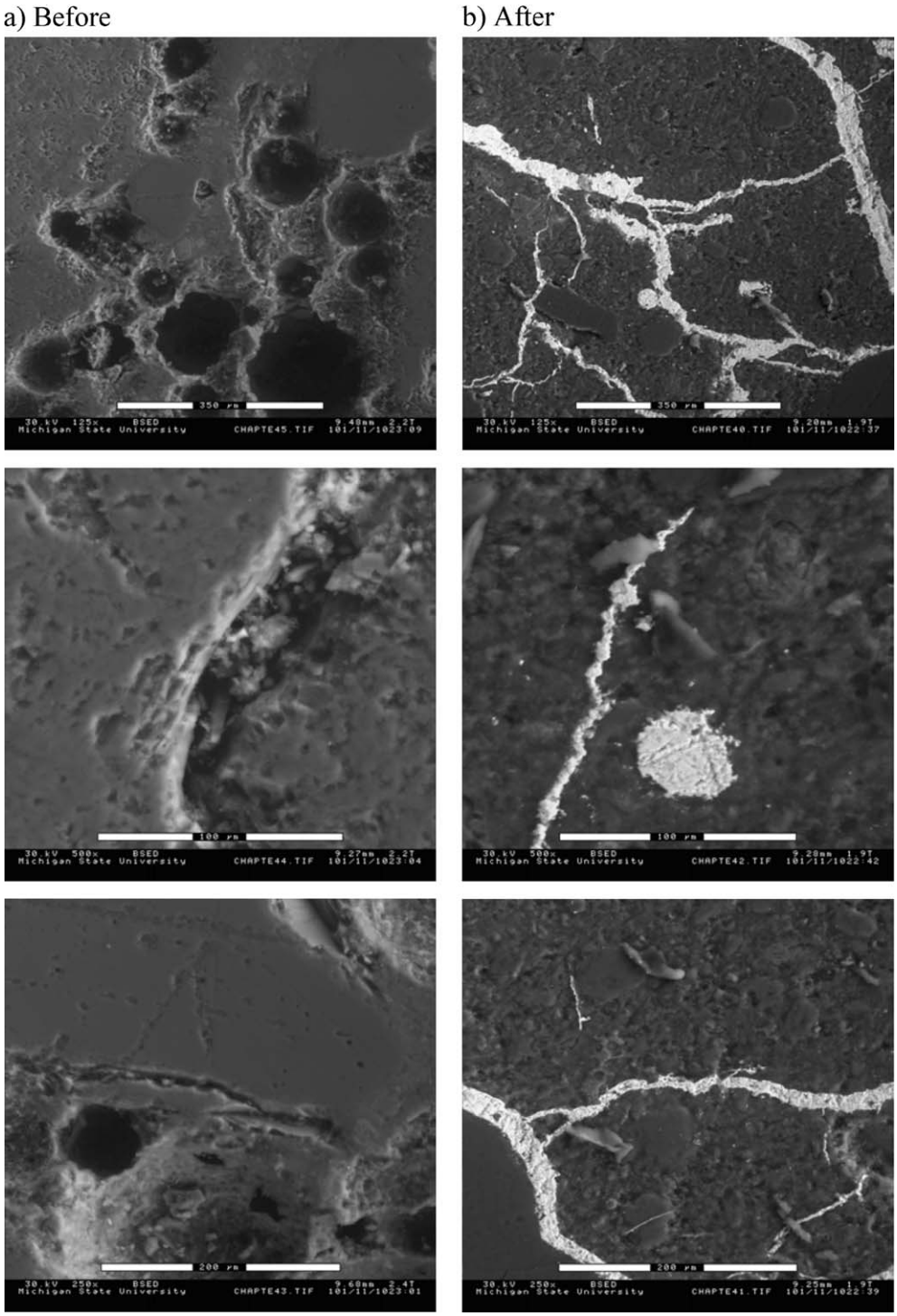

Fig. 3. Comparison between ESEM micrographs of concrete specimens before and after applying the proposed approach of specimen preparation.

Fig. 4. Allowing ink to immerse specimen.

carbide abrasive papers to obtain a smooth surface suiting ESEM investigation. A comparison between ESEM micrographs captured by backscattered technique for concrete specimens before and after applying the specimen preparation is shown in Fig. 3.

2.2. Specimen preparation for fluorescent microscopy (ink–epoxy impregnation)

Traditionally, fluorescent microscopic techniques have been employed for qualitative investigation of concrete materials impregnated with fluorescent epoxy. Conventional methods of fluorescent epoxy impregnation stain capillary pores as well as air voids and microcracks. It would thus be difficult to distinguish features of interest (microcracks and voids) from the body of concrete. A two-stage impregnation technique has been devised to resolve this problem. For this purpose, fine pores (capillary pores in hydrated cement paste and aggregate pores) are not first impregnated with black ink (Parker Quink); subsequently, microcracks and air voids are impregnated with fluorescent epoxy. The low viscosity of ink and its ability to harden in this thickness result in the filling of capillary pores but not microcracks and air voids in the first stage of impregnation. This two-stage impregnation yields a reasonable sharp contrast between features of interest (microcracks and voids) and body of concrete.

The first stage starts by cutting the specimen to 20–30-mm (0.8–1-in.) slices with the required cross-sectional dimensions using a suitable electrical saw (trying to maximize cross-sectional areas, given overall specimen dimensions and microscope travel stage dimensions). The specimen may be ground using a grinder in order to remove surface irregularities produced by the saw. During all the sawing and grinding operations, special care should be taken to keep specimen surfaces moist. One specimen surface is then lapped using an abrasive liquid comprising of 30 g (0.067 lb) vehicle 101 (Lapmaster Intl. Div.), 50 g (0.11 lb) aluminum oxide powder 1800, (Lapmaster Intl. Div.), and 450 g (0.99 lb) tap water under 0.021 MPa (3.0 psi) pressure. At the end of the lapping operation, the specimen should be carefully cleaned to remove any debris using a sponge with a 50% solution of an all-purpose cleaner followed by rinsing with water at low and then high speeds. The specimen should then be cleaned in ultrasonic bath (43 kHz frequency) for 20–30 min in order to remove any fine particles entrapped inside the voids or the microcracks. The specimen should be dried in oven at 60 °C (140 °F) for 3–4 h and then placed in a plastic container within a glass flask connected to the vacuum pump. Vacuum-drying of the specimen at 2.66 kPa (0.38 psi) for at least 1 h will substantially remove air from voids and microcracks. Vacuum is then turned, and from a container connected to the glass flask, black ink (60% by weight of Parker Quink–40% water) is allowed into the plastic container holding the specimen inside the flask in order to impregnate the specimen as shown in Fig. 4. The specimen is then moved to a pressure chamber (while kept immersed in ink and covered with a wooden plate in order to prevent splashing of ink when the pressure is introduced using nitrogen gas). The specimen should be subjected to nitrogen gas at a pressure of 1.94 MPa (280 psi) for 18–24 h in order to facilitate impregnation of the capillary pore system within cement paste (and aggregates) with ink. The final step in the first stage of sample preparation is to turn the pressure off, remove the sample from pressure chamber, and place it in oven at 60 °C (140 °F) for 24 h to dry the ink.

The second stage starts by placing the specimen in a plastic container within a glass flask connected to vacuum. The specimen should be subjected to the vacuum of 2.66 kPa (0.38 psi) for 1 h substantially to remove air from microcracks and voids. The fluorescent epoxy solution is prepared by adding 3.0 g (0.106 oz) of fluorescent dye (solvent yellow 43) (AAKASH Chemicals and Dye-Stuffs) to 30.6 g (0.0674 lb) (of "DER" 736 polyglycol diepoxide/epoxy resin) "modifier" and mixing them together, and then mixing 200 g (0.44lb) of "NSA" (455 ml noneylsuccinic

Fig. 5. Applying nitrogen pressure for epoxy penetration.

anhydride modified), followed by 76.8 of "ERL" 4221 vinylcyclophene dioxide "UC. D." "monomer" and 6 g (0.2 oz) of "DMAE" (2-dimethylaminoethanol) "epoxy accelerator-catalyst" (SPI-CHEM Supplies). The solution is poured in a glass container connected to a glass flask. After turning off the vacuum, the fluorescent epoxy is allowed to impregnate the specimen. With the specimen kept immersed in fluorescent epoxy, the specimen is placed in the pressure chamber and covered by a perforated wooden plate to prevent splashing of fluorescent epoxy dye when nitrogen pressure is applied. After closing the pressure chamber lid, the specimen is subjected to nitrogen

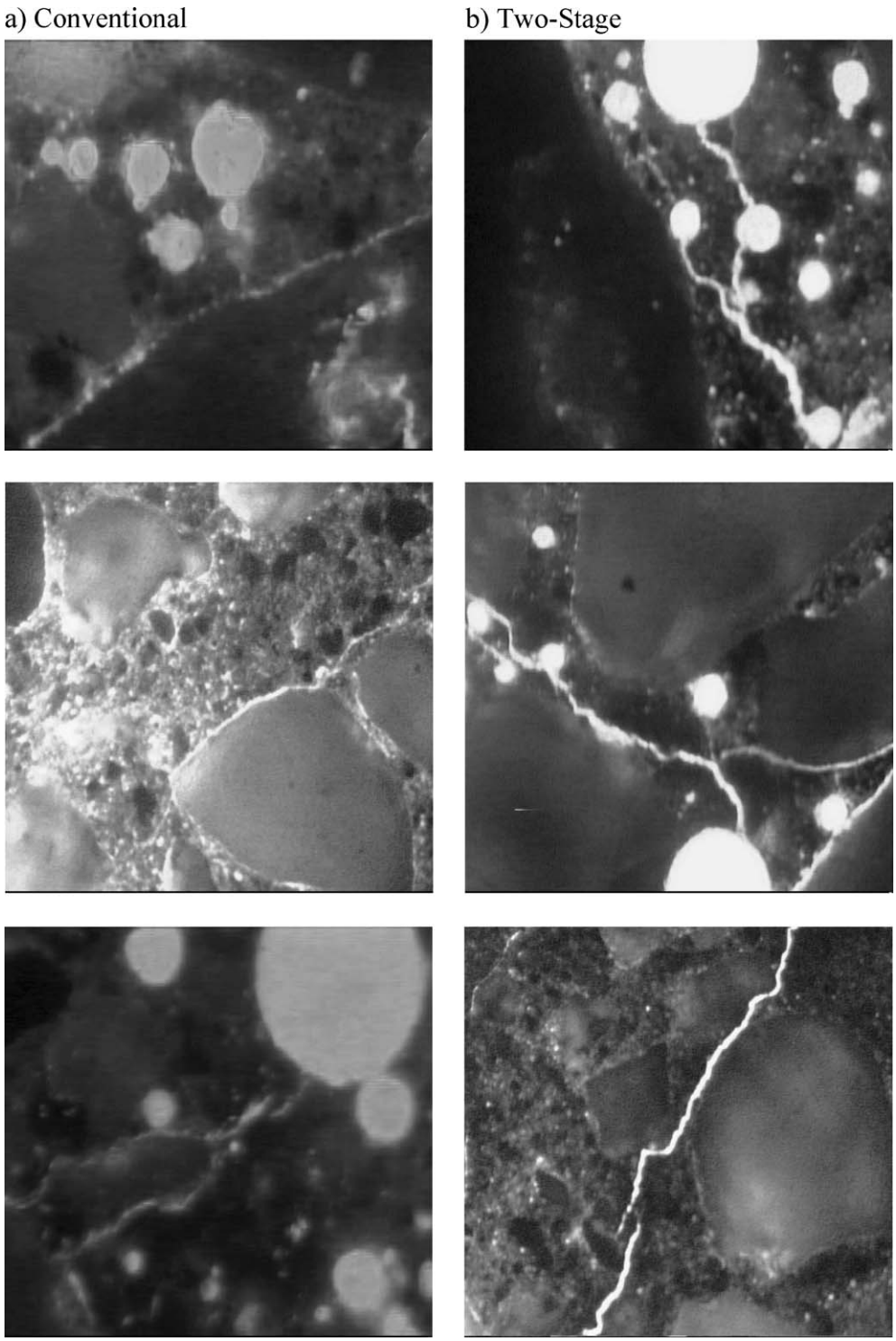

Fig. 6. Fluorescent micrographs of concrete specimens prepared by conventional and the new (two-stage) specimen preparation techniques.

Table 1
Comparison between manual and automatic low threshold levels for ESEM concrete micrographs

Comparison	Threshold function			
	Manual	Automatic		
		Factorization	Entropy	Moment
Minimum	101	107	68	73
Maximum	183	225	181	201
Mean	145	153	101	110
Standard deviation	27.7	23.9	26.6	21.8

pressure of 1.94 MPa (280 psi) for 3–4 h to allow for epoxy penetration into concrete microcracks and voids as shown in Fig. 5. The pressure is turned off, and the specimen is placed in the electrical oven at 65.5 °C (150 °F) for 18–24 h. The final step in the second stage is to lap the specimen surface using lapping machine and the previously described abrasive liquid under 0.021 MPa (3.0 psi) pressure to remove the thin film of the epoxy dye from the specimen surface to be ready for fluorescent microscopy investigation.

A comparison between concrete images prepared by conventional epoxy impregnation method and the proposed two-stage impregnation method is shown in Fig. 6.

3. Image processing techniques

3.1. Automated thresholding

Segmentation is a process through which the image is partitioned into meaningful regions based only on the intensity of the pixels. When segmentation is applied to a gray image, the gray level intensities of pixels which satisfy a given condition are set to one and the rest are set to zero. The converted image is referred to as a binary image where the pixels values can be presented by a single bit signaling a true or false situation (e.g., microcrack or not). Segmentation by brightness thresholding is the simplest approach where a contrast gray level is used as the threshold value; therefore, it is widely used to convert a gray scale image to binary (black and white) images. In the simplest version of brightness discrimination, there are two threshold methods (manual and automatic) and three different types of thresholding (by factorization, entropy, moment) [13]. From the automation

Table 2
Comparison between manual and automatic low threshold levels for fluorescent concrete micrographs

Comparison	Threshold function			
	Manual	Automatic		
		Factorization	Entropy	Moment
Minimum value	76	88	99	61
Maximum value	201	238	244	241
Mean value	186	197	222	165
Standard deviation	31.2	33.7	38.8	35.6

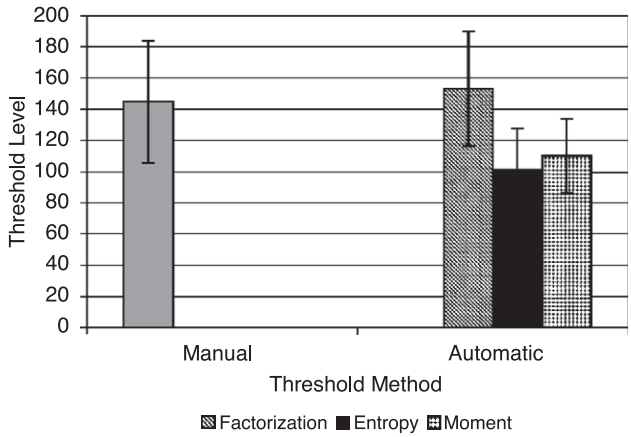

Fig. 7. Threshold levels for both manual and automatic threshold functions for ESEM concrete micrographs.

point of view, manual thresholding is not applicable due to the large variations in gray-scale level between images; therefore, a comparative study is generally performed to check the possibility of using automatic (in lieu of manual) thresholding and also to determine the suitable auto-threshold type for particular circumstances (e.g., particular specimen preparation and microscopy techniques).

In this investigation, 100 images (containing microcracks and voids) were captured from specimens prepared by the pre-described specimen preparation techniques using both ESEM and fluorescent microscopy at different magnifications (125 ×, 250 ×, and 500 ×); these images were used as training set, using both manual and automatic thresholding functions as applied. The low threshold level was set to zero (default value) for automatic thresholding, and the best threshold level image was determined. Throughout manual threshold, the optimum high threshold level was determined by comparing the original "gray" image and the image after application of manual threshold on "binary" image. When the features of interest (microcracks and

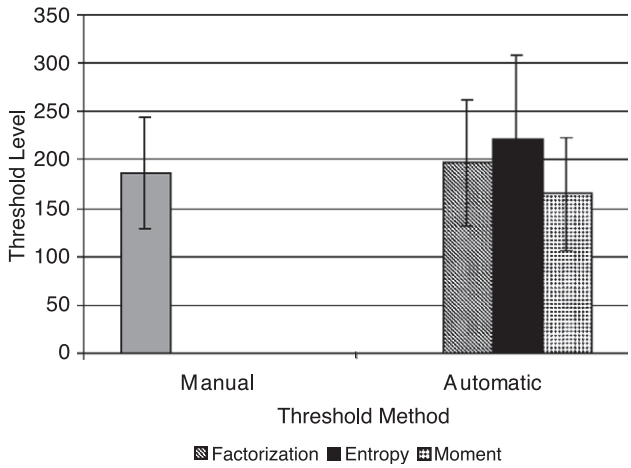

Fig. 8. Threshold levels for both manual and automatic threshold functions for fluorescent concrete micrographs.

voids) were correctly highlighted, the most distinct contrast between microcracks/voids and the concrete background was obtained. Three different automatic threshold functions were applied on the same image, yielding the high threshold level for each function. Tables 1 and 2 and Figs. 7 and 8 summarize the results of this comparative study. Statistical analysis (comparison of means) between the low gray level of manual threshold function and the three types of automatic threshold functions showed that there is no significant difference between manual threshold and automatic threshold (factorization) function for both ESEM and fluorescent micrographs. Statistical analysis also indicated that there is a significant difference between manual threshold and automatic threshold (entropy and moment) at 5% and 2%

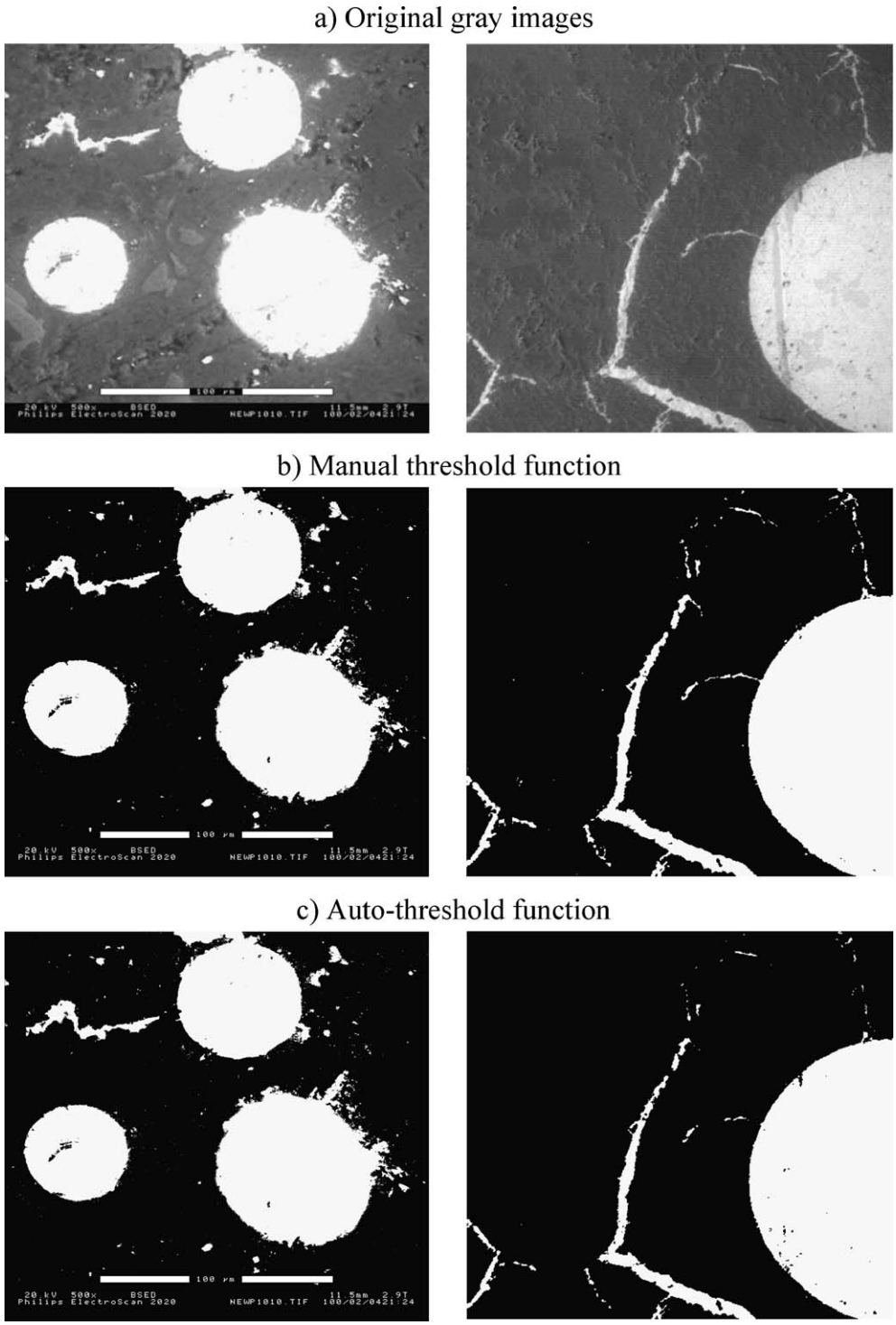

Fig. 9. Comparison between manual and automatic (factorization) threshold function on ESEM concrete micrographs.

levels of significance, respectively, for ESEM micrographs and at 9% and 2% levels of significance for fluorescent micrographs.

Effects of applying manual and automatic (factorization for ESEM micrographs and entropy for fluorescent micrographs) threshold functions on some of the captured images are shown in Figs. 9 and 10.

3.2. Detachment of intersecting and/or connected microcracks and voids

In few cases, some concrete microcracks and voids could intersect, and some concrete voids could also be attached. Measurements such as perimeter, crack width, and void diameter could be inaccurate if such connected features are

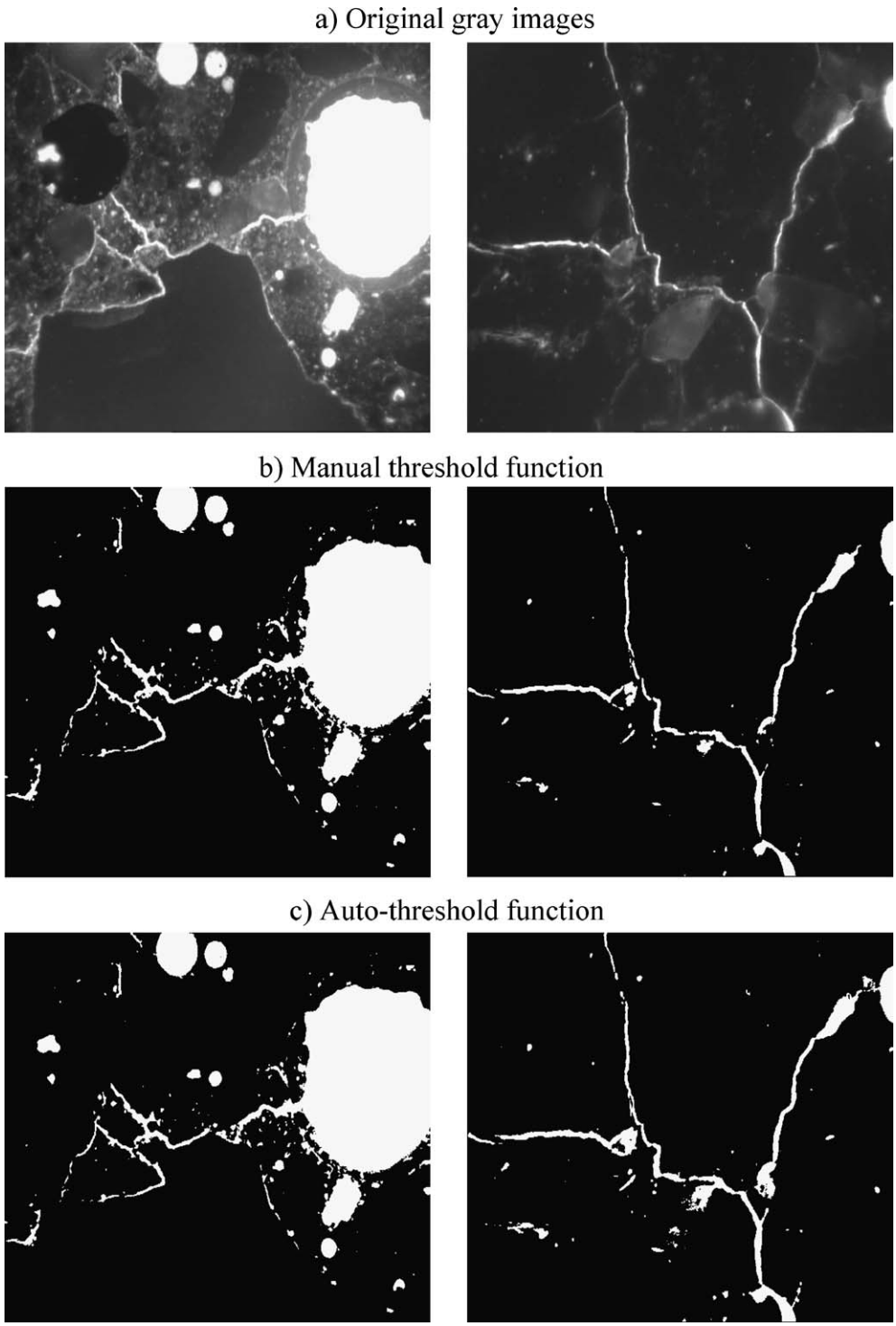

Fig. 10. Comparison between manual and automatic (factorization) threshold function on fluorescent concrete micrographs.

not detached. An image processing scenario had been developed to detach connected and intersecting features. This scenario begins with application of the ''opening'' operation on the original (gray) image (Fig. 11a) with large number of iterations (about 10) in order to remove microcracks and produce an image with only voids (Fig. 11b); the point operation function ''arithmetic-subtract'' is applied to create another image containing the removed microcracks (Fig. 11c). The ''opening'' function may be applied on the microcrack image with small number of iterations (about 3) for the purpose of noise removal. The next step is to apply the ''erosion'' function on the voids image in order followed by

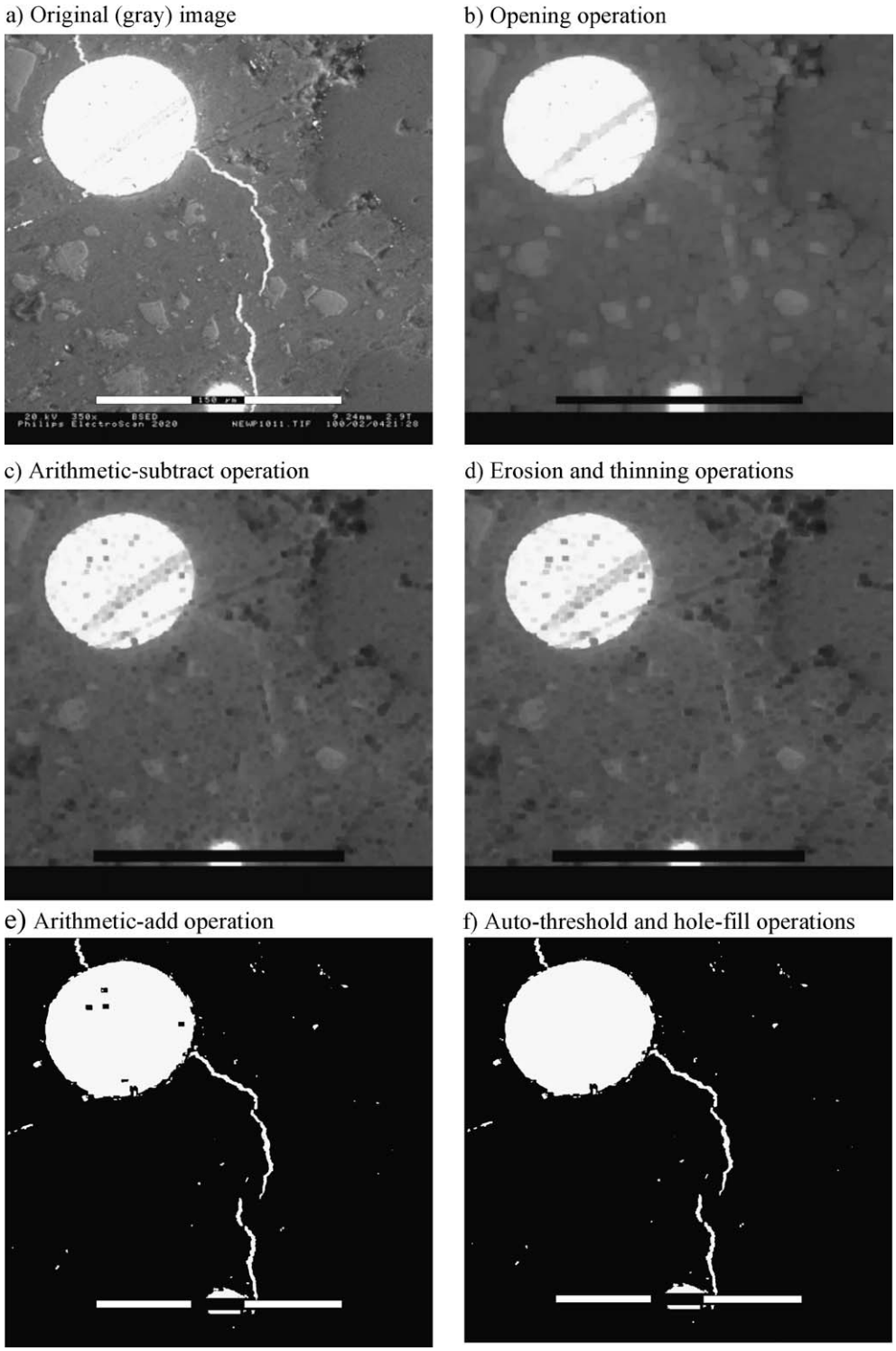

Fig. 11. Image processing scenario for detachment of intersecting microcracks and voids.

the "thinning" operation by using "Ierode Kernel" with a relatively large number of iterations (about 8) (Fig. 11d). The "thinning" operation is meant to remove some pixels, which connect cracks with voids, around voids without a noticeable loss of feature area. The point operation function "arithmetic-add" is then applied to reconstruct the original image again (Fig. 11e), yielding an image very similar to the original image (gray) one where connected/intersecting features have been detached. The "auto-threshold" function can be applied on the resulting image in order to transform it to a binary scale image. Subsequently, the "closing" function may be applied in order to compensate for some of the removed pixels.

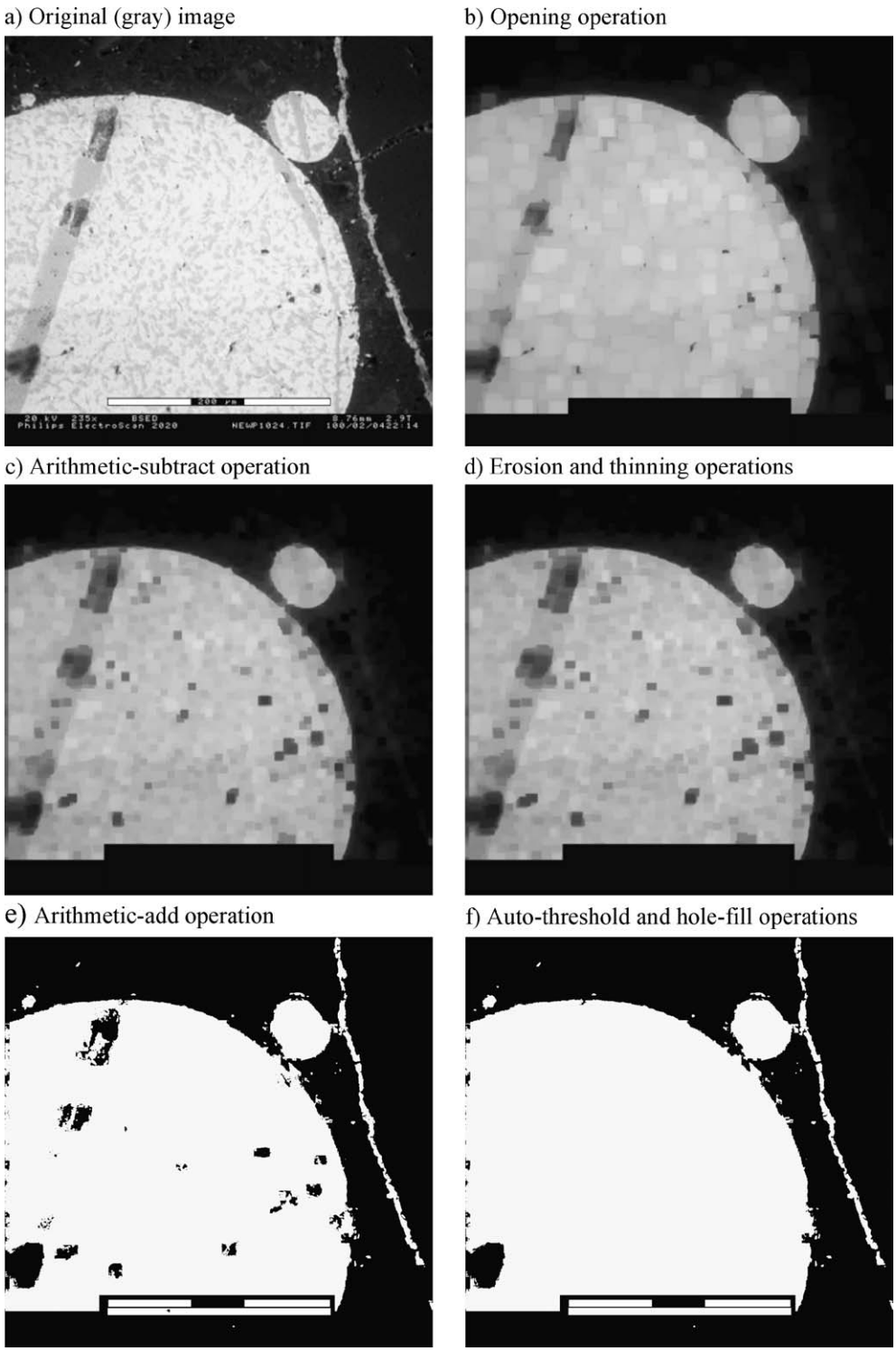

Fig. 12. Image processing scenario for detachment of intersecting microcracks and voids as well as connected voids.

Table 3
Statistical summary of formfactor measurements for microcracks and voids

Statistics	Formfactor values	
	Microcracks	Voids
Mean	73.044	1.3829
Median	80.23	1.114
Minimum value	5.6463	1.0
Maximum value	107.1	2.9631

Finally, the "hole-fill" function can be applied to fill the empty holes created in voids by the "erosion operation" (Fig. 11f). Fig. 12 presents another application of the image processing scenario to detach intersecting microcracks and voids as well as connected voids.

4. Image analysis techniques

4.1. The criterion to distinguish between microcracks and voids (shape analysis)

Microcracks and air voids are key microstructural features of concrete which can be resolved through microscopy. Microcracks and voids have different effects on engineering properties; efforts to quantify these two features should thus start with distinction of microcracks from voids; their key attributes can then be quantified separately.

The shape of objects is recognized in complex ways by our visual system. Instead of using numerical values, human being's eyes rotate objects to the same orientation before making comparisons and distinguishing different objects. A particularly interesting and revealing characteristic of the visual matching of patterns occurs when similar objects are viewed in different orientations. The length of time required to make a decision as to whether objects are the same is directly proportional to their angular deviation [14]. The proposed approach, however, distinguishes microcracks from voids quantitatively, based on distinct aspects of their geometry.

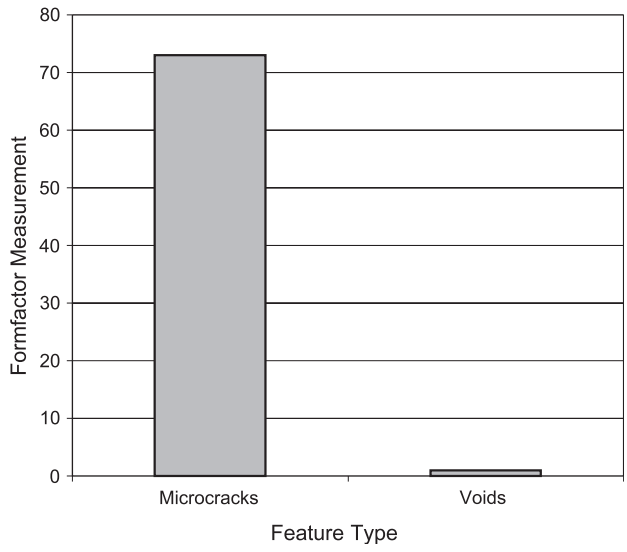

Fig. 13. Comparison between formfactor measurement for microcracks and voids.

Table 4
Visual vs. automated measurements of microcracks and voids

Statistics	Proposed criterion		Visual distinguishing		Error (%)	
	Microcracks	Voids	Microcracks	Voids	Microcracks	Voids
Number	132	307	141	298	−6.38	+3.02
Formfactor						
Mean	33.3	2.22	35.7	1.99	−6.6	+11.4
Minimum	3.64	1.01	3.53	1.01	+3.32	0.0
Maximum	44.7	1.63	44.7	1.58	0.0	+3.03

Microcracks, when compared with voids, are elongated features with relatively high aspect (length-to-width) ratios. A "formfactor" ("shapefactor") which distinguishes microcracks from voids is as follows:

$$\text{formfactor} = \frac{\text{length of the object}}{\text{width of the object}} \quad (1)$$

In order to determine the threshold value of formfactor (above which the object is a microcrack), 300 (environmental scanning electron and fluorescent) microscopic images of concrete were used as the training image set. The images were captured at different magnifications ($\times 125$, $\times 250$, and $\times 500$), using different concrete mixes. Microcracks and voids were distinguished visually; their corresponding formfactors (aspect ratios) were measured using a standard (Visilog 5.3) image analysis software.

A total of 471 microcracks and 1172 voids were analyzed in the 300 selected images. A summary of the formfactor measurements is presented in Table 3. Fig. 13 presents the mean values of formfactor measurements for microcracks and voids. Based on these measurements, the formfactor of 3.5 was selected as the limit which distinguishes between microcracks and voids. Microcracks are considered to have

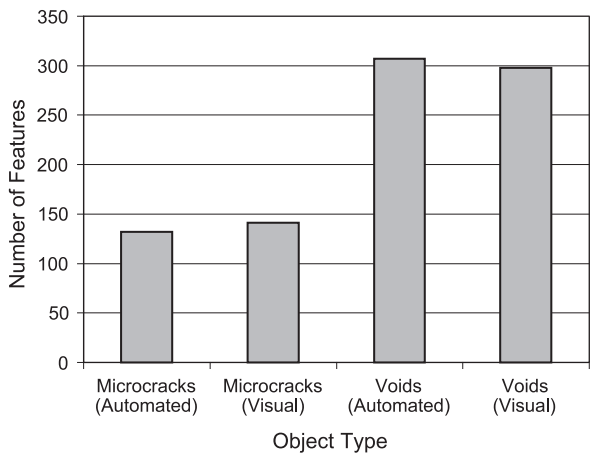

Fig. 14. Visual vs. automated formfactor measurements.

Table 5
Lengths of noise, microcracks, and voids at the three different magnification factors

Length (pixels)	125× magnification			250× magnification			500× magnification		
	Noise	Microcracks	Voids	Noise	Microcracks	Voids	Noise	Microcracks	Voids
Minimum	2	18.4	8	2.82	29	6.72	2	29	35.5
Maximum	106	478	612	82	756	906	165	948	745
Mean	15.5	97.7	107	16.8	130	205	24.4	198	271

Table 6
The errors (%) associated with different threshold length values for distinguishing noise

Threshold (length)	125× magnification			250× magnification			500× magnification		
	Noise	Microcracks	Voids	Noise	Microcracks	Voids	Noise	Microcracks	Voids
25 pixels	20.9	5.95	22	21.5	1.61	22.2	28.8	1.78	2.10
30 pixels	8.14	8.33	22	14.2	1.75	22.2	24.2	1.88	1.13
35 pixels	7.55	11.9	22	4.93	7.0	25.9	19.9	1.88	1.25

formfactor values greater than or equal to 3.5, while voids are considered to have formfactor values less than 3.5.

In order to validate the proposed criterion for distinction of microcracks form voids, the approach was applied to another training set of 100 images which included a total number of 439 microcracks and voids. Table 4 and Fig. 14 compare the automated and visual counts of microcracks and voids. The number of automatically distinguished microcracks and voids differ from the visually identified ones by 6.38% and 3.02%, respectively. These differences are considered to be reasonably small in light of the advantages of automated approach in terms of efficiency and speed of operations.

4.2. The criterion for noise removal (size analysis)

Despite all precautions during specimen preparation, there is still a large probability that captured images may contain noise from different sources. Noise can result from leftover impregnating agent on the surface of the lapped specimen, uneven distribution of light under microscope, improper adjustment of the brightness and contrast of microscope, or improperly impregnated microcracks and voids. Image processing functions can be employed to remove most (but not all) of the noise. In order to complement the noise removal effect of image processing, a criterion is developed here to identify noise based on its

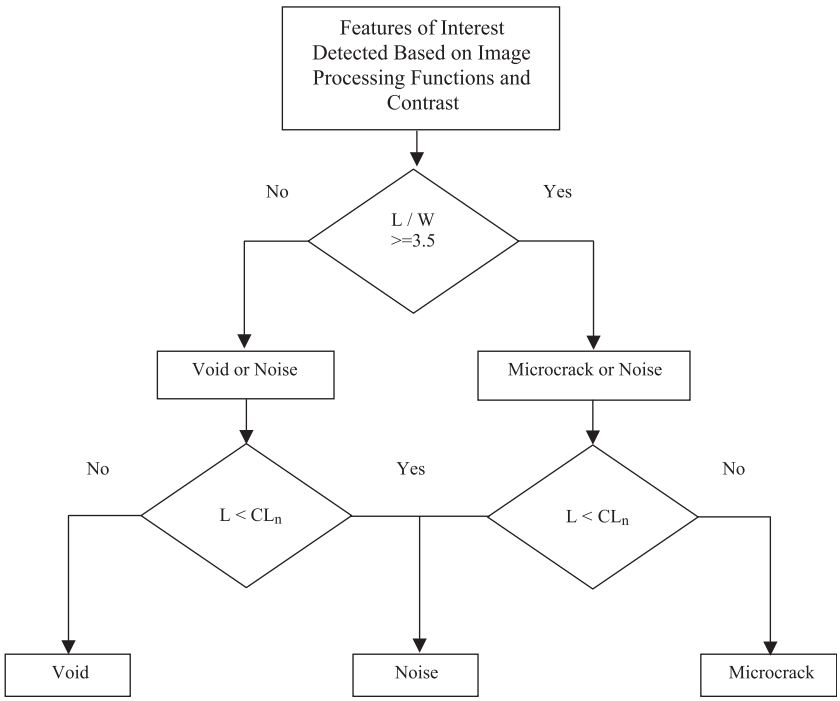

Fig. 15. Flowchart presentation of the criteria for distinction of microcracks, voids, and noise.

distinctly small size when compared with features of interest (microcracks and voids).

After evaluating different size and shape variables, the length (the largest dimension) was chosen to distinguish noise from microcracks and voids. Length measurements at three different magnifications (using 150 training images for each magnification) are summarized in Table 5 (noise, microcracks, and voids were identified visually in this case). Size analysis indicated that features smaller than about 30 pixels in length are mostly noise; this threshold number of pixels can range from 25 to 35. Errors in distinguishing noise for different threshold number of pixels (as well as errors in identifying microcracks and voids) are introduced in Table 6. Depending on the magnification factor (and probably sample preparation conditions), the threshold length (in number of pixels) for distinguishing noise from microcracks and voids should be selected based on visual observations of the impact of such noise removal criteria on the images.

The criteria introduced above for distinction of microcracks from voids and also noise from features of interest are summarized in Fig. 15. Notations (L) and (W) refer to the length and width of features, respectively, and (CL_n) refers to the selected critical length of noise in pixels (for distinguishing noise from microcracks and voids).

5. Summary and conclusions

Automated quantitative microstructural analysis of concrete microcracks and voids systems requires proper selection of image processing operations complemented with appropriate sample preparation techniques which highlight microcracks and voids against the body of the concrete. The accomplishments and conclusions of the study are summarized below.

1. A refined specimen preparation technique was developed to prepare concrete specimens for SEM investigation by Wood's metal impregnation. A new two-stage specimen preparation method was developed to prepare concrete specimens for fluorescent microscopy investigation. This two-stage approaches first impregnates concrete with ink, which is cured to fill capillary pores; subsequently, microcracks and voids are impregnated with fluorescent epoxy dye.
2. Automatic threshold schemes best suiting automated identification of microcracks and voids in prepared concrete specimens were identified; these schemes greatly facilitate automation of concrete microstructural analysis.
3. Image processing scenarios were developed for detachment of intersecting microcracks and voids and also separation connected voids for accurate quantification of concrete microcrack and void system.
4. Image analysis schemes were developed to distinguish between microcracks and voids and to identify noise in concrete microscopy images. Formfactor (length–width ratio) of "3.5" was found to distinguish microcracks from voids at magnifications 125 ×, 250 ×, and 500 ×. Recognizing and filtering out noise (produced due to poor specimen preparation and/or setting of instrumentation) from concrete micrographs was carried out by comparing the length of features of interest with noise and addressing the critical length of the noise. The critical length ranged from 25 to 35 pixels based upon the used magnification factor.

Notations

SEM (conventional) scanning electron microscopy
ESEM environmental scanning electron microscopy
L length of feature
W width of feature
CL_n critical length of noise in pixels

Acknowledgements

The work reported herein was conducted jointly by DPD and Michigan State University, under the sponsorship of the US Air Force.

References

[1] S. Mindess, Interfaces in concrete: materials science of concrete I, in: J. Skalny (Ed.), Material Science of Concrete, vol. 1. The American Ceramic Society, USA, 1989, pp. 163–180.
[2] A. Helmuth, The nature of concrete: significance of tests and properties of concrete and concrete-making materials, in: P. Klieger, J. Lamond (Eds.), Fly Ash in Cement and Concrete, ASTM Pub., USA, 1994, pp. 5–14.
[3] D. St. John, A. Polle, I. Sims, Concrete Petrography, Wiley, 1998, pp. 10–46.
[4] J. Russ, Image analysis of the microstructure of materials: images of materials, in: B.W. David, R.P. Alan, G. Ronald (Eds.), Image of Materials, Oxford Univ. Press, 1991, pp. 338–373.
[5] J. Russ, Computer-assisted microscopy, the measurement and analysis of images, Plenum, New York, NY, USA (1990) 20–25, 105–115, and 134–148.
[6] S. Marusin, Sample preparation—the key to ESM studied of failed concrete, Cem. Concr. Compos. 17 (4) (1995) 311–318.
[7] A. Amouche, J. Riss, D. Greysse, J. Marchand, Image analysis for the automated study of microcracks in concrete, Cem. Concr. Compos. 23 (2/3) (2001) 267–278.
[8] H. Hornain, J. Marchand, A. Ammouche, J. Commene, M. Moranville, Microscopic observation of cracks in concrete—a new sample preparation technique using dye impregnation, Cem. Concr. Res. 26 (4) (1996) 573–583.
[9] K. Nemati, J. Monteiro, K. Scrivener, analysis of compressive stress-induced cracks in concrete, ACI Mater. J. 98 (5) (1998) 617–630.

[10] P. Stutzman, Specimen preparation, [online] Available, http://www.cee.ce.uiuc.edu/lange/micro, 1999.
[11] H. Gran, Fluorescent liquid replacement technique. A means of crack detection and water: binder ratio determination in high strength concretes, Cem. Concr. Res. 25 (5) (1995) 1063–1074.
[12] Materials safety data sheet, Goodfellow company.
[13] M. Coster, J. Chermant, Image analysis and mathematical morphology for civil engineering materials, Cem. Concr. Compos. 23 (2/3) (2001) 133–151.
[14] J. Russ, The Image Processing Handbook, CRC Press, New York, NY, USA, 1992, pp. 1–7.